

# A 3D channel body interpretation via multiple attributes and supervoxel graph cut

Xingmiao Yao<sup>1</sup>, Mengxin Zhang<sup>1</sup>, Mengyang Sun<sup>1</sup>, Cheng Zhou<sup>1</sup>, Yang Yi<sup>1</sup>, and Guangmin Hu<sup>1</sup>

## Abstract

Channels have always been vital geologic features in the exploration of hydrocarbon reservoirs, which makes the interpretation of channels an important task. Many different seismic attributes have been proposed to help the process of channel interpretation. A single seismic attribute could not fully and accurately reflect the geologic structure and edge details of a channel. Therefore, interpretation on a single attribute causes inaccurate segmentation. A 3D channel body interpretation method based on multiple attributes and supervoxel graph cut is applied in this paper, which identifies and segments the channel geologic body with fuzzy boundaries, poor continuity, or even data loss more accurately. First, a nonlinear dimensionality reduction method (locally linear embedding with geodesic distance) is applied to fuse a variety of seismic attributes to make channels clearer. Then, a graph-cut method based on the super geologic voxel is introduced, which reduces the computational complexity of segmentation and generates supervoxels more fitted to the edge of the channel body. Finally, a smooth 3D surface of the channel is obtained through the isosurface extraction. We use the data of a work area in northwest China and Parihaka-3D to evaluate the performance of our method. Our results show that, compared with other methods, the information provided by the fusion attribute is more complete, and the edge continuity of the channel is improved. The 3D channel bodies obtained by our method are clear and continuous. In the case of a complex channel body, our method can also work well.

## Introduction

The interpretation of 3D models of geologic bodies is one of the most important tasks in the interpretation of seismic data because most of the important hydrocarbon reservoirs exist around geologic bodies. The 3D model of a geologic body visually represents its structural shape and distribution in the 3D space and enables the interpreter to perform quantitative analysis for the geologic body. The 3D model of a geologic body also provides momentous reference for the reservoir numerical simulation, reserve calculation, and well location deployment.

Edge detection methods are commonly used in the detection of geologic bodies. Zhou et al. (2007) use an edge detection method to identify the boundary of the salt dome, but the results are not ideal due to noise in seismic data. Aqrabi et al. (2011) propose a method that combines 3D edge detectors and tilt-angle steering for detecting geologic bodies, thus improving the signal-to-noise ratio and edge continuity and making the boundary shape of geologic bodies clearer. However, edge-based methods heavily depend on amplitude changes. For example, there may be unsatisfactory results when the instantaneous amplitude of the edge does not change

significantly. To reduce the dependence on amplitude, a geologic body recognition method based on texture attributes was proposed. Berthelot et al. (2013) use a set of texture properties to predict the probability that each pixel in a 3D cube belongs to a salt dome, and then they find the boundaries of the salt dome by segmentation. Shafiq et al. (2015) use a texture gradient to detect the boundaries of the salt dome through the large variation in gradient at the edges. However, the texture-based method is not universal for different work areas because the size of the windows has a great influence on the results. Amin and Deriche (2015) propose a hybrid approach for salt dome detection for better detecting salt domes, which combines the advantages of the edge method and the texture method. Di et al. (2017) further combine the three attributes of edge detection, geometry, and texture, and they perform semiautomatic fault detection using a support vector machine. Alfarraj et al. (2018) explore the application of multiresolution analysis techniques as texture attributes in seismic image characterization, especially in the subsurface structural characterization of large-scale seismic data. Long et al. (2018) compare the typical texture attributes presented in the image processing literature, and they discuss how

<sup>1</sup>University of Electronic Science and Technology of China, Chengdu, China. E-mail: yxm@uestc.edu.cn (corresponding author); 201722010827@std.uestc.edu.cn; sehuntering@163.com; zhoucheng@std.uestc.edu.cn; 13547844973@163.com; hgm@uestc.edu.cn.

Manuscript received by the Editor 13 September 2018; revised manuscript received 14 April 2019; published ahead of production 12 June 2019; published online 9 September 2019. This paper appears in *Interpretation*, Vol. 7, No. 4 (November 2019); p. T739–T749, 12 FIGS., 3 TABLES.

<http://dx.doi.org/10.1190/INT-2018-0158.1>. © 2019 Society of Exploration Geophysicists and American Association of Petroleum Geologists. All rights reserved.

to use the texture attributes to calculate and characterize the subsurface geologic structures in the seismic volume. Wu (2017) proposes using directional tensors to improve seismic coherence images to show clearer, more continuous fault and stratigraphic features. Wu and Guo (2019) further propose a diffusion scheme that iteratively smoothens a seismic image along reflections and channels while updating the mappings of faults and channels. This scheme is designed to detect faults and channels while enhancing seismic structural and stratigraphic features.

However, unlike salt domes and caves, channels do not have obvious and definite boundaries on a certain attribute data, especially amplitude data. Furthermore, the channels are curved and have poor continuity. Therefore, the above methods for identifying and segmenting the geologic bodies are not well applied to the channel segmentation.

Many scholars segment channels from the perspective of seismic attributes. Seismic attributes are data sets extracted from the original 3D seismic data by a certain algorithm. Seismic attributes reflect the characteristics of seismic data from different perspectives. Different geologic structures show different characteristics in attribute values. Suarez et al. (2008) first use the seismic attributes to assist the analysis of the channel body. Through a comparative analysis of multiple seismic attribute slice charts, the channel boundary was comprehensively divided. However, the signal-to-noise ratio of the data greatly affects the resolution and quality of seismic attributes, and some seismic attributes do not contribute to the division of the channel. Zhang et al. (2011) apply the RGB multiattribute fusion technique to channel identification to make the edges of the channel clearer and to improve the resolution. Chia et al. (2014) decompose the seismic attributes into three frequency bands by coherence and spectral decomposition, which were represented by different colors, and then visualized by RGB fusion. This method identified channels quickly and effectively. However, RGB fusion is only suitable for integrating three attributes, and it is not applicable when more attributes need to be fused. Meanwhile, most research studies only use visual techniques to assist subjective judgment and do not segment the boundary of the channel body qualitatively.

Image-based methods are equally applicable to channel segmentation, and many scholars have tried to solve the channel segmentation problem from the perspective of computer vision. To solve the problems of complex structure and poor continuity of channels, Mathewson and Hale (2009) enhance the local linear characteristics of the channel through the method of the steerable pyramid in image processing. Kadlec et al. (2008) propose a confidence level and curvature-guided level set method to segment the channel body from 3D seismic data. Boustani et al. (2019) propose to use a curvelet transform and morphological filter to map channel edges in seismic data. Liu et al. (2016), on the basis of the fusion of various seismic attributes, use a level set

method to segment various geologic bodies such as caverns and channels. However, methods that are based on the level set are more dependent on the initial shape and have low computational efficiency. Karbalali et al. (2017) propose channel boundary detection based on 2D shearlet transformation. The edge candidates could be found based on maximizing the shearlet coefficients on the horizontal and vertical cones for all shearing directions at each pixel location for the finest scale of decomposition. Pham et al. (2018) apply deep learning to channel detection. They train the network on a 3D synthetic data set using SegNet and Bayesian SegNet architecture borrowed from computer vision and then apply it to field data.

In general, most of the existing studies for channel identification and detection are on the 2D surface, and studies for constructing the 3D models of channels are insufficient. Segmentation methods based on supervoxels and graph cut have been successfully applied to many image processing problems (Kitrunrotsakul et al. 2015; Tian et al. 2015). Considering that, we propose a method for channel segmentation by supervoxel graph cut on the basis of multiattribute fusion. First, we integrate a variety of seismic attributes to obtain a new seismic data volume, and then we use a graph-cut method based on supervoxels to binarize the channel. The locally linear embedding with geodesic distance (ISOLLE) algorithm is adopted to enhance the fusion of seismic attributes. The supervoxel is used to overcome poor pixel edge retention. Finally, a 3D surface of the channel is extracted through the isosurface.

The main innovations of this paper are

- 1) The ISOLLE algorithm is first applied to multiattribute fusion of 3D seismic data, which can describe the nonlinear relationship of seismic data. The introduction of geodesic distance in ISOLLE makes the fusion result more comprehensive and accurate.
- 2) The super geologic voxel is first combined with the graph-cut algorithm to obtain more continuous channel's segmentation results.

## Methods

The flowchart of the proposed approach is illustrated in Figure 1. First, a variety of attributes are selected from the original amplitude data volume according to the attribute category and the sensitivity to the channel body. Then, these attributes are merged into new attributes by the ISOLLE algorithm. Based on the data of these new attributes, super geologic voxels are generated by a simple linear iteration (simple linear iterative cluster [SLIC]) method. The graph-cut algorithm is then used for channel segmentation. The segmentation of the channel is converted into an energy function minimization problem by constructing an energy function, a segment based on minimum cut criterion, and output binarized 3D data. Finally, by extracting isosurfaces, a 3D model of the channel geologic body is obtained.

## Geophysical attribute fusion based on ISOLLE

In the process of seismic interpretation, different attribute data describe the geologic structure from different aspects. By combining different attributes, the geologic structure of the reservoir is explained more precisely. Many methods have been proposed for the integration of multiple seismic attributes. Le and Wang (2002) apply cluster analysis to attribute fusion. Qi and Zhang (2012) introduce seismic multiattribute fusion based on the D-S evidence theory to predict the concentration of coalbed methane (CBM). Córdoba et al. (2012) use principal component analysis (PCA) for attributes of fusion of fault, which greatly improved the accuracy of microfault recognition. Shi et al. (2018) propose a geotechnical industrial fracture identification framework that used seismic anisotropy and multisensitive properties to automatically integrate different fracture types in the reservoir. Wu et al. (2018) propose a seismic multiattribute reservoir quantitative prediction method based on sedimentary subregions, which provides a new idea for reservoir prediction.

Because the relationship between seismic attributes and geologic features is usually nonlinear, the PCA method based on linear transformation does not fully capture this nonlinear relationship, which reduces the accuracy of prediction and recognition. Liu et al. (2010) use a nonlinear locally linear embedding (LLE) algorithm to achieve the feature extraction of layers for the first time. However, the LLE dimensionality reduction algorithm uses a Euclidean distance that is unable to reflect the true structure between points and is sensitive to the choice of the number of neighbors.

The ISOLLE (Varini et al., 2006) algorithm combines the ideas of ISOMAP (Balasubramanian and Schwartz, 2002) with LLE. Replacing Euclidean distances with geodesic distances maintains the advantage of the LLE algorithm for processing high-dimensional data, while improving the tightness of data and the linear characteristics of local neighborhood data in the corresponding low-dimensional space. The ISOLLE method is applied to multiattribute fusion of 3D channel seismic data. The data set is  $X = \{x_1, x_2, \dots, x_N\} \in R^{M \times N}$ , where the attribute value of the  $i$ th point is  $x_i = [x_i^1, x_i^2, \dots, x_i^M]^T$ . The Euclidean distance  $d_E(x_i, x_j)$  between two points  $x_i$  and  $x_j$  is expressed as

$$d_E(x_i, x_j) = \sqrt{(x_i - x_j)^T (x_i - x_j)}. \quad (1)$$

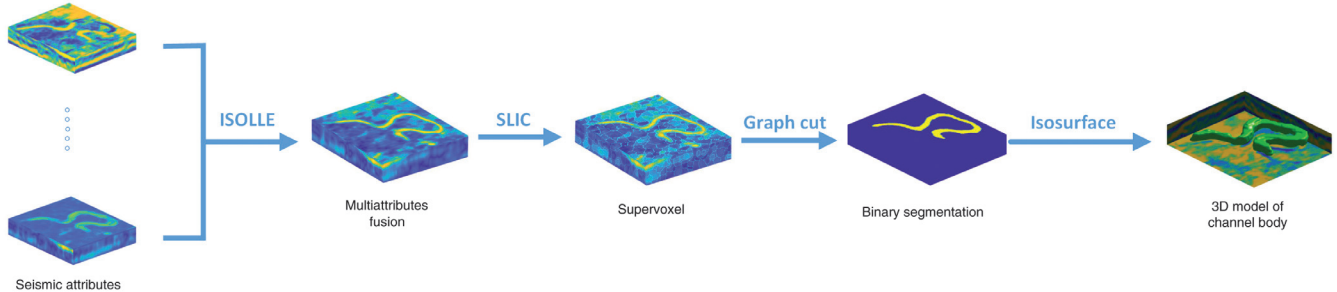


**Figure 1.** Flowchart of segmentation and 3D modeling of the channel body.

Suppose there is a path  $U = \{x_i, \dots, x_j\}$  between sample points  $x_i$  and  $x_j$  and  $|U|$  indicates the number of elements in the path, then, the path length  $L_G^U(x_i, x_j)$  between the two points is as shown in formula 2:

$$L_G^U(x_i, x_j) = \sum_{r=1}^{|U|-1} d_E(U_{(r)}, U_{(r+1)}). \quad (2)$$

Therefore, for two points  $x_i$  and  $x_j$  where there are multiple paths  $\{U_1, U_2, \dots, U_m\}$ , their geodesic distance  $d_G(x_i, x_j)$  is as shown in formula 3:

$$d_G(x_i, x_j) = \min_{r=1, \dots, m} \{L_G^{U_r}(x_i, x_j)\}. \quad (3)$$

Based on the principle of geologic attribute optimization proposed by Varini et al. (2005), the root-mean-square amplitude attribute, energy attribute, texture homogeneity, spectrum attribute, and instantaneous frequency attribute are selected to study multiattribute fusion in a seismic engineering area in northwest China. The pseudocode of the algorithm is shown in Algorithm 1, where  $I_k$  represents a  $k$ -dimensional column vector that all elements are one. After normalization and Fourier transform denoising, slice diagrams with different attributes are obtained, as shown in Figure 2. Different attributes on the same time slices could make up for each other's deficiencies.

The result of the fusion for a given neighbor points is shown in Figure 3, where  $k$  is the number of neighbors. When the value of  $k$  is small, the fusion result is not ideal, and it is not possible to distinguish the inside and outside of the channel clearly. In general, we set the value of  $k$  to be 10–15, so that we can maintain the local linear relationship better and embed the high-dimensional spatial relationship between multiple attributes into a merged low-dimensional space. Compared with each slice of seismic attributes in Figure 2, the new physical properties after fusion show the boundaries of the channel geology more continuously and clearly.

## Supervoxel graph-cut algorithm to segment the channel body

Pixel-level segmentation does not take full advantage of the local relationships between pixels, which would introduce errors in the process of image discretization.

Superpixels (Wang et al., 2011) use the similarity of features between pixels to group pixels. A small number of superpixels instead of a large number of pixels is used to express image features. Compared with pixel-level segmentation, superpixels preserve the edge features of the original image. Supervoxels (Veksler et al., 2010) are an extension of superpixels in 3D space.

#### Algorithm 1. Using ISOLLE to fuse multiple seismic attributes.

- ① For  $x_i$  of  $N$  data set  $X = \{x_1, x_2, \dots, x_N\} \in R^{M \times N}$ , compute the geodesic distance between other data points with  $x_i$
  - ② Select  $k$  data points  $X_i = \{x_1, x_2, \dots, x_k\} \in R^{M \times k}$  that have the smallest geodesic distance with  $x_i$
  - ③ From  $k$  data points of  $x_i$ , we generate the locally reconstructed weight matrix:
- $$Q^i = \begin{pmatrix} (x_i - x_{i1})^T \\ \vdots \\ (x_i - x_{ik})^T \end{pmatrix} ((x_i - x_{i1}), \dots, (x_i - x_{ik}))$$
- ④ Compute local optimization reconstruction weight matrix  $w_i = \frac{(Q^i)^{-1} \cdot I_k}{I_k^T (Q^i)^{-1} I_k} \in R^{k \times 1}$
  - ⑤ Obtain the sparse matrix  $W_i$  of  $w_i$  to make  $x_i = \sum_{j=1}^N W_{ij} x_j$
  - ⑥ From  $N$  points, we generate  $D = (W_1, W_2, \dots, W_N)$  optimization reconstruction weight matrix0
  - ⑦ Compute the feature vectors  $Y = \{y_1, y_2, \dots, y_N\} \in R^{N \times 1}$  of  $L = (I - D)(I - D)^T$ , which is the value of fused multiple seismic attributes

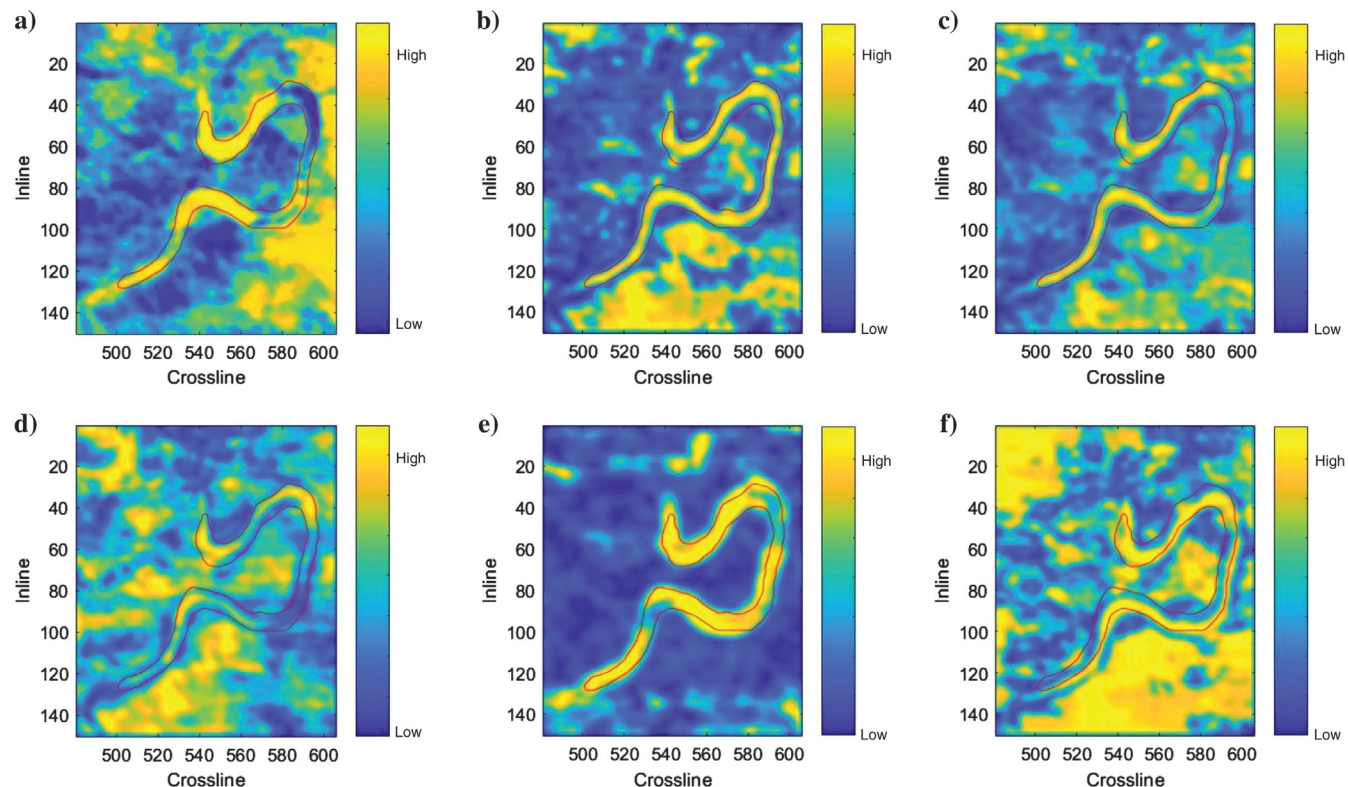


**Figure 2.** (a) Original amplitude attribute, (b) energy attribute, (c) rms amplitude attribute, (d) frequency attribute, (e) texture attribute, and (f) frequency filter attribute.

When dealing with 3D seismic data, the method of super geologic voxels overcomes the problem of unsMOOTHNESS in the final synthesis of 3D models when using superpixels on 2D slices, and it reduces the number of blocks and the amount of computation.

However, supervoxels coarsely segment the image. Therefore, the graph-cut algorithm is introduced to further perform fine segmentation based on super geologic voxels. In image processing, the method based on the graph cut (Boykov and Jolly, 2001) has been effectively used in many problems. For example, Lin et al. (2006) use the model-based graph cut method in medical images to implement the segmentation of the left ventricle successfully. Cha et al. (2018) combine supervoxels with the graph cut for the segmentation of computed tomography images. The final results are very close to the edges obtained by manual interpretation, and they are superior to the existing 3D segmentation methods in accuracy and time complexity.

#### SLIC algorithm to generate super geologic voxels

The SLIC algorithm is used to generate superpixels, and the algorithm has been widely applied in the field of computer

vision (Chen et al., 2018). The edge of the pixel block generated by this method is cleaner and smoother, and the intersection area between image blocks is easy to express, which makes the method easier to use with other methods. In seismic volumes, the closer the two seismic data points are, the greater is the probability that they belong to the same geologic body. According to this feature, we cluster similar seismic data points based on the SLIC algorithm (Achanta et al., 2012) to generate super geologic voxels. The generated super geologic voxels keep the interior uniform and compact and maintain the edge characteristics of the geologic body, which reduces the computational complexity of subsequent segmentation. In the SLIC algorithm, the main steps are to compare the distance between each point and the cluster center  $C$  for classification, and then update the cluster center. The pseudocode of the algorithm is shown in Algorithm 2. For all  $K$  cluster centers  $C_j (j = 1, 2, 3, \dots, K)$ , in the neighborhood of  $2S \times 2S \times 2S$ , the distance from each point to the cluster center  $C_j$  is shown in formula 4:

$$d_{ij} = \sqrt{d_g^2 + \left(\frac{d_{xyz}}{S}\right)^2 m^2}, \quad (4)$$

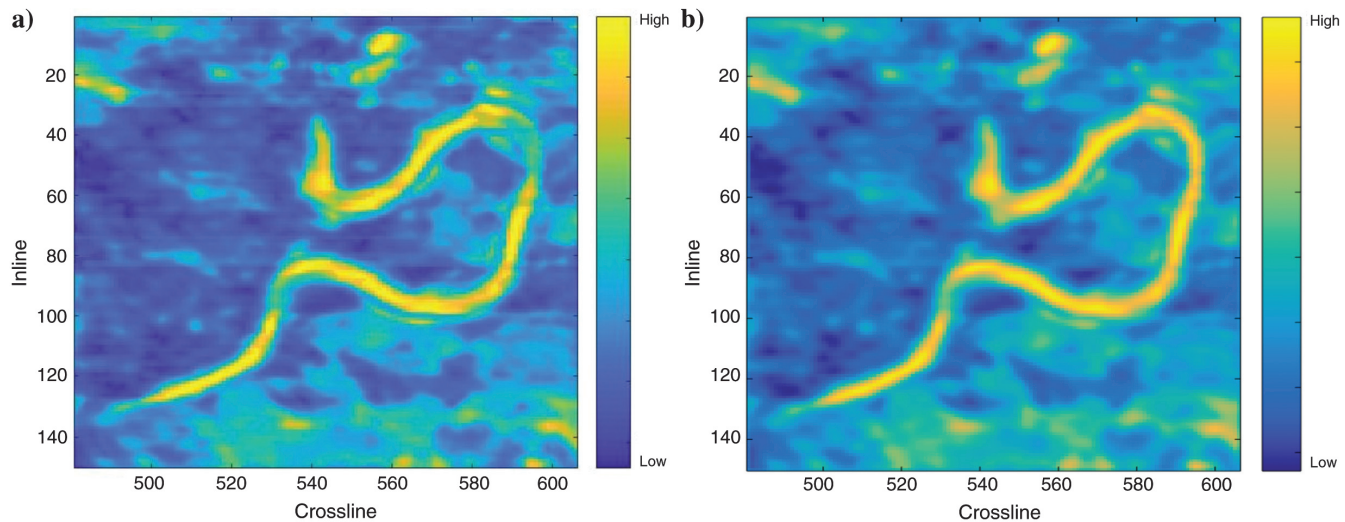


**Figure 3.** Fusion results when the number of neighboring points  $k$  is equal to 10,12.

#### Algorithm 2. Generating super geologic voxels with SLIC.

- ① Initialization: Generate  $K$  seed points and  $K$  is the number of super geologic voxels
- ② Calculate the distance from each point to  $C_j$  in the  $2S \times 2S \times 2S$  neighborhood of the cluster center  $C_j$
- ③ Update the cluster center  $C'_j = \frac{\sum_{\text{label}_i=j} v_i}{N_j}$ , where  $N_j$  is the number of seismic data points belonging to the  $j$ th super geographic voxel and  $\text{label}_i$  is the label value of the  $i$ th point
- ④ Repeat execution ③ until  $E = \sum_{j=1}^K C'_j - C_j$  is less than the threshold or exceeds the number of iterations
- ⑤ For super geologic voxels whose volume is not greater than the threshold, calculate the Bahrain distance between it and the neighboring supervoxels and merge them into the adjacent supervoxels with the smallest distance

where  $d_g = \sqrt{(g_i - g_j)^2}$  is the distance between the seismic data point  $i$  and the clustering center  $C_j$  in the merged attribute data and  $g_i$  is the attribute value of seismic data point  $i$ . The term  $d_x = \sqrt{(x_i - x_j)^2 + (y_i - y_j)^2 + (z_i - z_j)^2}$  is the Euclidean distance between the seismic data point and the cluster center  $C_j$  in the 3D space, and  $m$  is the parameter to adjust weight of distance and space, which is usually taken as one.

Figure 4 shows that the segmented super geologic voxels do not fit enough at the edge of the channel when the number of super geologic voxels  $K$  is small. When  $K$  is large, the distinction between the inside and outside of the channel is ambiguous, and the method does not effectively reduce the computational burden of graph cut. Therefore, we set the number  $K$  of supervoxels to 150, which allows the segmented super geologic voxels to fit the edge of the channel well and makes the homogeneity of the super geologic voxels better.

#### Segmentation of channel geologic body based on the graph cut

The geologic supervoxels contain some texture features. Therefore, the supervoxel-based graph-cut algo-

rithm is applied to the segmentation of channel geology. On the basis of the traditional graph segmentation algorithm, we represent the value of each supervoxel by the fusion of attribute values. Compared to the traditional graph-cut algorithm, this paper uses the Gaussian mixture model (GMM) (Bond et al., 2001) instead of the histogram to accurately express the probability model. The core of the GMM is to find the mean, variance, and weight ratio of each of its Gaussian components. First, the GMM is initialized by K-means method, and then it is iteratively optimized by the expectation–maximization algorithm, and, finally, the GMM of the channel geologic body is obtained. The pseudocode of the algorithm is shown in Algorithm 3.

The gray-level co-occurrence matrix is the joint probability distribution of two gray values in the image (Bo et al., 2006). In this paper, the gray-level co-occurrence matrix is used to calculate the texture properties of each super geometry voxel. Five attributes are selected as the eigenvalues of supervoxels, including energy, frequency filter, texture, instantaneous frequency, and rms amplitude. We replace the original single data points by the segmented super geologic voxels, and we finally segment the channel geologic body with the graph-cut algorithm (Chen and Bagci, 2011). The pseudocode of the algorithm is shown in Algorithm 3.

## Results

The experimental data are a 3D field seismic data set containing information of channel body in northwest China, with a data volume of  $3.65 \times 3$  km.

Figure 5 shows four seismic attributes fusion results by PCA, LLE, ISOMAP, and

---

### Algorithm 3. Graph cut based on super geologic voxel.

---

- ① Manually mark supervoxels of the channel body as  $\alpha_i = 1$ , others as  $\alpha_i = 0$
  - ② Repeat
    - Carry out K-means clustering on super geologic voxels
    - Update channel and nonchannel GMM parameters based on clustering results
    - Use the graph-cut algorithm to construct a graph and energy function
    - Segment geologic data based on the max-flow min-cut theorem
    - Update channel and nonchannel supervoxels markers  $\alpha_i$
    - until result convergence or the maximum number of iterations
  - ③ Output the binary segmentation result of the channel geology body.
- 

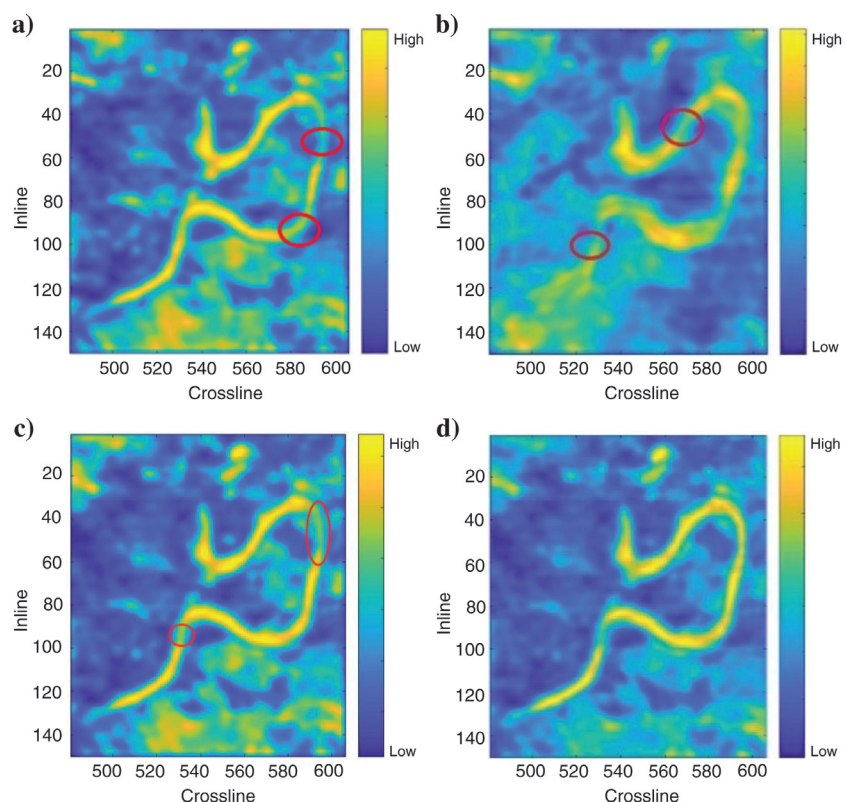


**Figure 5.** The fusion results of multiseismic attributes using the PCA, LLE, ISOMAP, and ISOLLE methods when  $k = 12$  and  $t = 15$  ms.

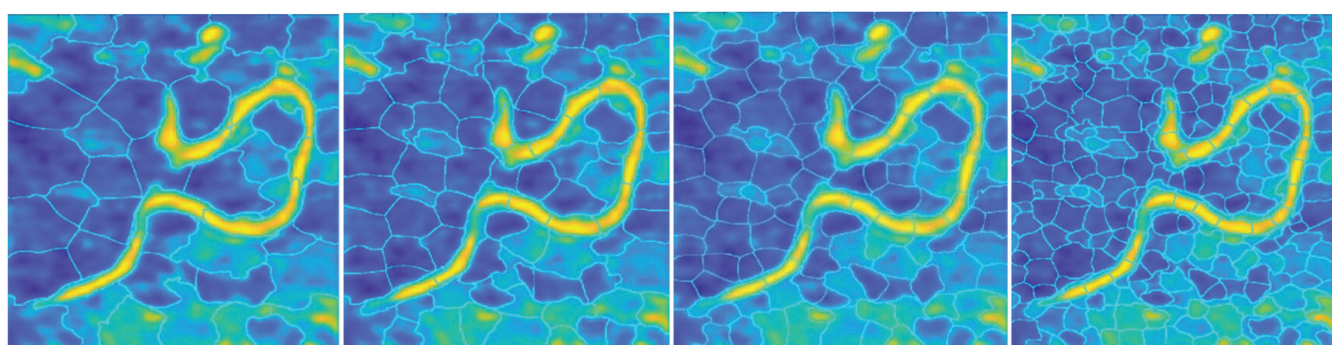


**Figure 4.** Supervoxel segmentation results when  $k$  is equal to 50, 100, 150, and 300.

ISOLLE. Figure 5 shows that although the LLE fusion method takes the same number of neighboring points as the ISOLLE method, the channel is not accurately segmented due to the uneven distribution of the seismic data. Although the effect of fusion between PCA and ISO-MAP is better than that of the single attribute, the continuity of the channel is weaker than that of the ISOLLE method, and the unevenness of the grayscale of the channel is more serious. The edge of the channel segmented by the ISOLLE method is clearer and more continuous. The new attribute obtained by the fusion of the ISOLLE method has a higher signal-to-noise ratio and retains the linearly separable features of the neighborhood, making the boundary of the channel clearer. With the advantages of the previously selected seismic attributes, the merged attributes improve the signal-to-noise ratio of the image and characterize the channel more accurately and comprehensively with more detailed features. Figure 6 shows the seismic data profile and the channel boundary on the time slice.

The accuracy of the results is analyzed by a 2D slice diagram, as shown in Figure 7. From the original amplitude (Figure 7a), the edge of the channel is blurred with poor continuity. The ISOLLE method (Figure 7b) integrates seismic attributes such as energy, frequency filter, texture, instantaneous frequency, and rms amplitude to make the edges of the channel clearer, the difference between the inside and outside of the channel more apparent, and the internal homogeneity of the channel strength-

ened. Through the segmentation method based on super-voxels and the graph-cut proposed in this paper, the binarization segmentation result (Figure 7c) is obtained. In general, the edge obtained in Figure 7c is the same as the result obtained by the geologic interpreter (Figure 7d).

For further evaluating the segmentation results, the same data are segmented by the segmentation method of regional growth and level set. The results are shown

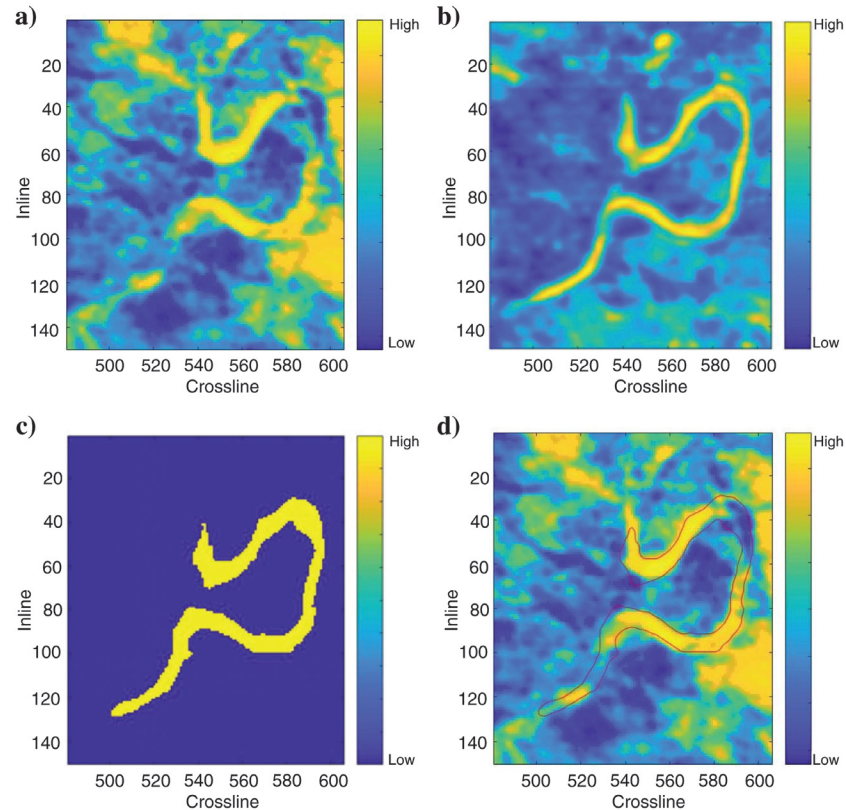


**Figure 7.** Slice containing 3D seismic data of channel information at time 15 ms.

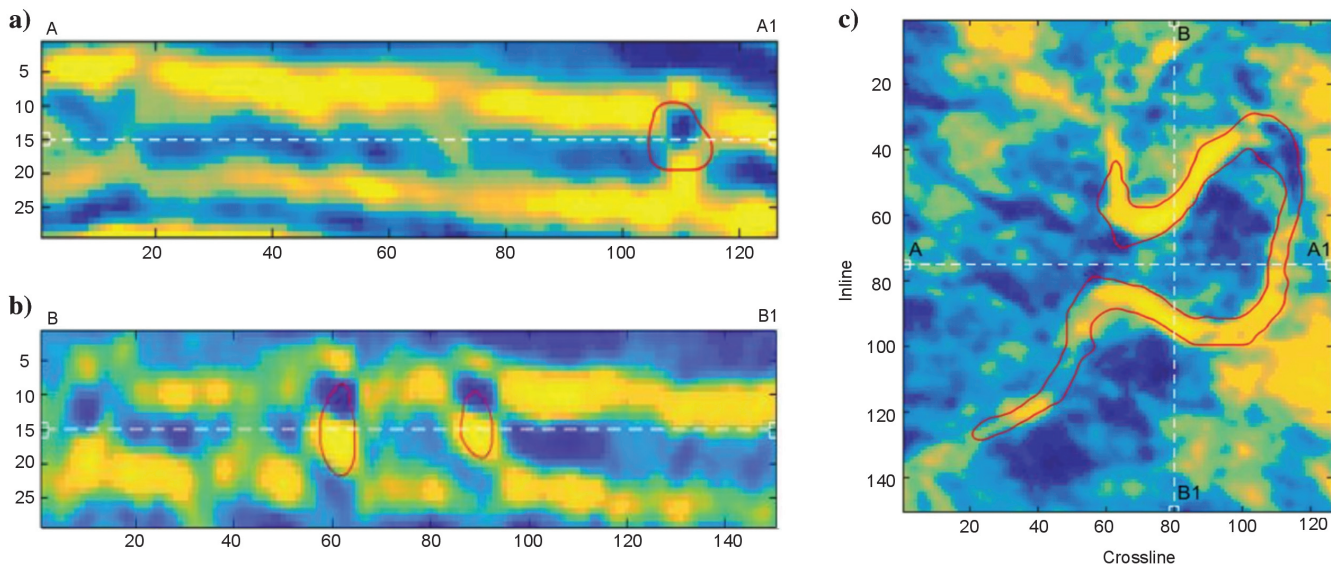


**Figure 6.** Seismic data section and channel boundaries on the time slice (the solid red line).

in Figure 8. The false fraction (FF) and true positive fraction (TPF) (Fenster and Chiu, 2005) are used to quantitatively evaluate the effects of the above methods. If  $V_s$  and  $V_T$  represent the segmented channel area and the real channel area, respectively, these two performance indicators are written as formulas 5 and 6. The term “ $\cap$ ” represents the AND operation, and “ $\oplus$ ” represents the XOR operation:

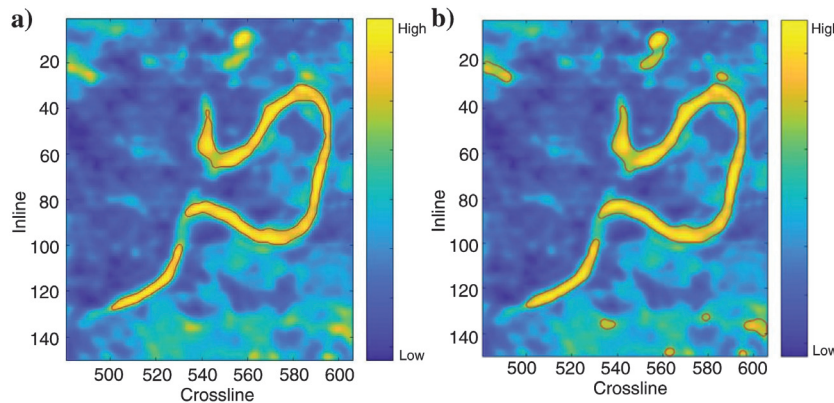


**Figure 8.** (a) Region growth segmentation results and (b) level set segmentation results.

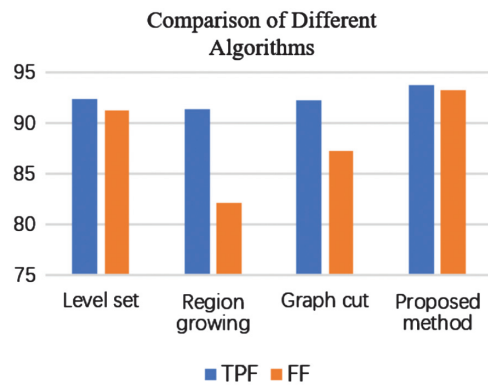


**Figure 9.** Comparison of different algorithms.

$$\text{TPF} = \frac{V_S \cap V_T}{V_T}, \quad (5)$$

$$\text{FF} = 1 - \frac{V_S \oplus V_T}{V_T}. \quad (6)$$

The region growing method does not extract a continuous target body from the original data due to gray unevenness in the channel data. The method of level set segmentation seeks the boundary of the channel by establishing the energy function of the image and minimizing the energy function. For the same data, the division of the level set does not inhibit the segmentation of other nonchannel areas and has poor continuity.

Figure 9 shows the TPF and FF indicators for the level set, region growth, graph cut, and our method. It can be seen that our method has achieved the best TPF and FF and has greatly improved the accuracy.

After the binary operation of the channel, the channel surface is obtained by isosurface extraction and the isovalue is taken as zero. The 3D model of the channel geologic body is shown in Figure 10.

To verify our method further, we select another 3D seismic data to detect and segment channel. These 3D seismic data are a subset extracted from the 1520 km<sup>2</sup> Parihaka 3D seismic survey located at the Taranaki Basin, a broad sedimentary basin on the western side of the North Island, New Zealand. The field seismic data set covers an area of 10.81 × 8.35 km. Due to the large data set, we cluster the data set for preprocessing first, which can reduce the data volume and help to strengthen the continuity of segmentation. Figure 11 shows five attributes and the fusion attribute of the Parihaka data. The new fusion attribute is obtained by ISOLLE. It can

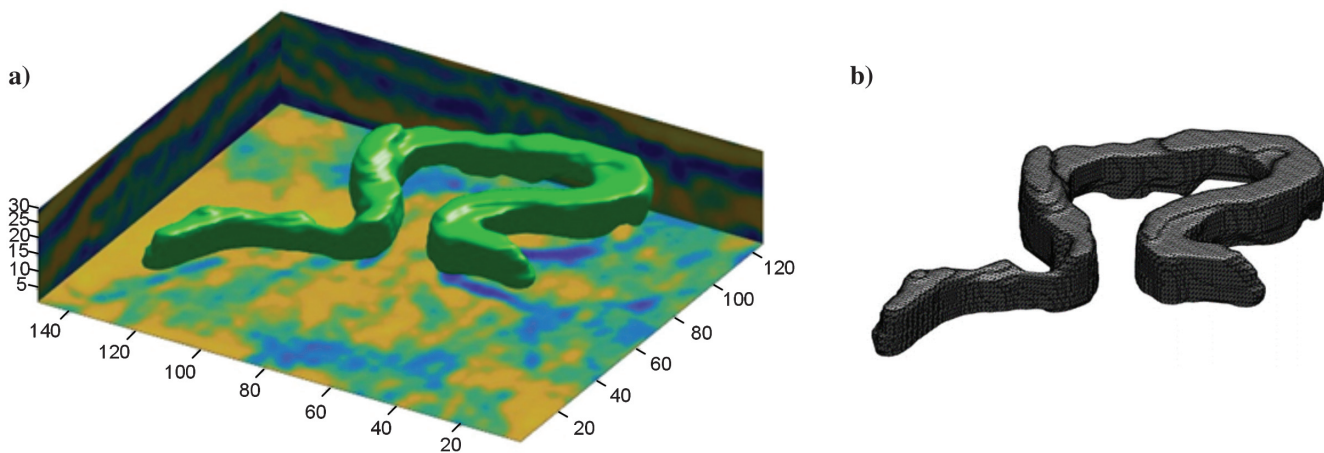


**Figure 10.** The 3D model of the channel body.

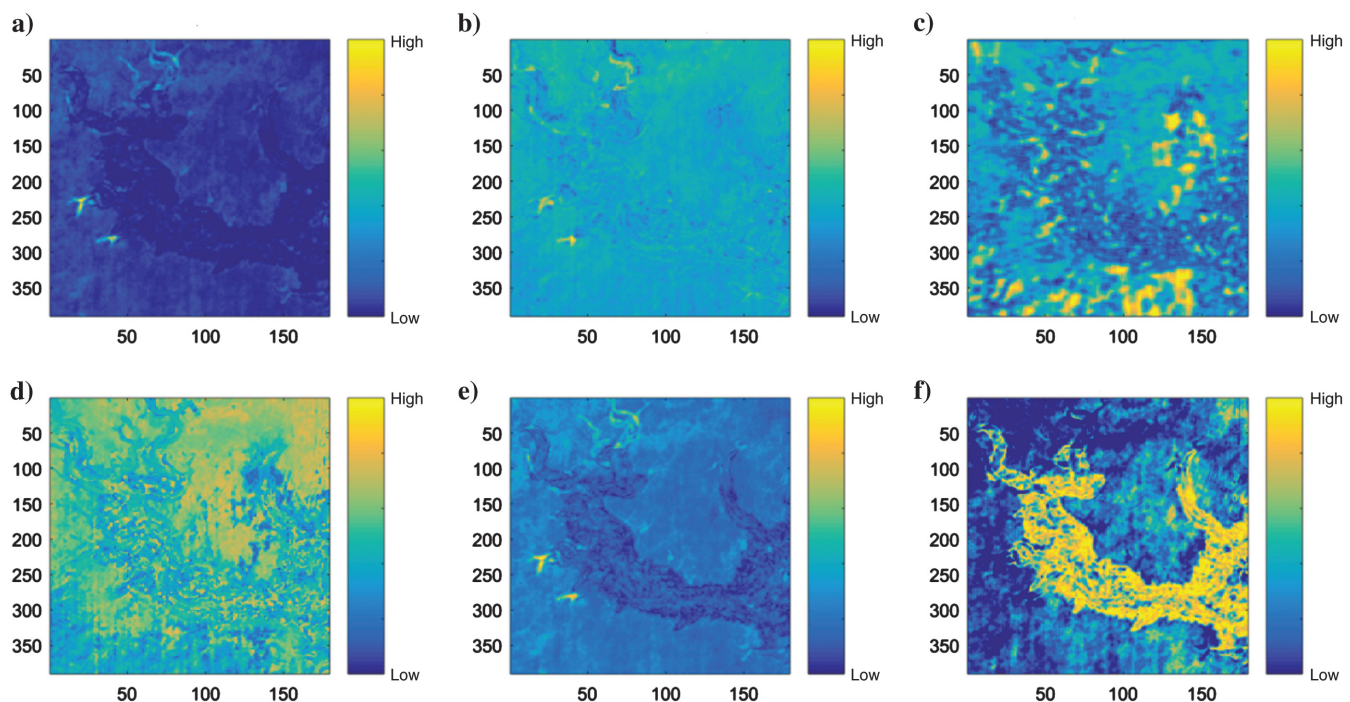


**Figure 11.** (a) Energy attribute, (b) frequency filter attribute, (c) texture attribute, (d) frequency attribute, (e) rms amplitude attribute, and (f) fusion attribute by ISOLLE.

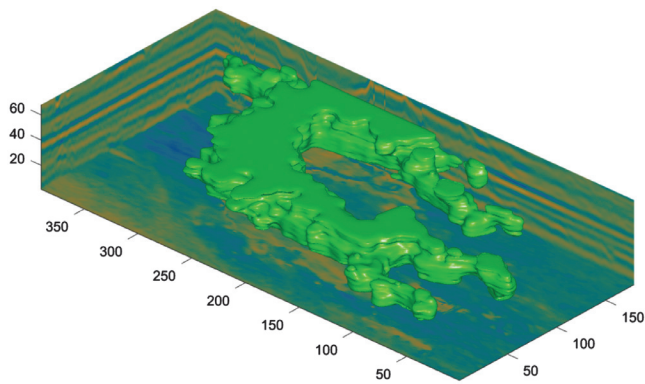


**Figure 12.** The 3D channel model of the Parihaka data set.

be seen that the channel in the fusion attribute has better continuity. The distinction between channel and non-channel in the fusion attribute is also more obvious than that in the other five attributes. The 3D model of the channel geologic body is shown in Figure 12. It shows that the method of this paper can still segment the channel accurately when the channel structure is more complicated.

## Conclusion

To construct the 3D model of the channel geologic body more accurately, a method based on multiattribute fusion and supervoxel graph cut is proposed to segment the channel geologic body and build the 3D model. A new data volume is obtained by merging several preferred seismic attributes. It is then binarized and segmented by the supervoxel graph-cut method.

Finally, the surface of the channel body is extracted from the isosurface. The experimental results show:

- 1) The characteristics of a single seismic attribute to the channel are often not comprehensive enough, which makes the segmentation results deviate from the actual boundary of the channel. Consequently, the final 3D model of the channel geologic body does not accurately reflect its characteristics. Reasonable selection of seismic attributes helps to complement information and characterize the channel's geologic body more fully.
- 2) The ISOLLE fusion method integrates multiple seismic attributes effectively. The multiattribute fusion method maintains the nonlinear relationship in the seismic data of the channel, and the new attribute data body obtained has laid a good foundation for the next step of segmentation and reconstruction.
- 3) Super geologic voxels combined with graph cut have good edge retention segment channels accurately and quickly. The 3D model of channel geologic bodies obtained from 3D seismic data through isosurface extraction demonstrates the spatial characteristics of the channel geologic body more intuitively.
- 4) The proposed method based on multiple attributes and the supervoxel graph cut realizes the accurate delineation of the channel geologic body. The generated 3D model conforms to the geologic rules and is basically consistent with the results explained by geologists and lays a foundation for the follow-up work.

## Acknowledgments

This research is supported by the National Natural Science Foundation of China (NSFC) grant no. U1562218. The authors thank the geophysical experts of the Sichuan Chuanqing Geophysical Technology Co. Ltd for their help with the geologic interpretation. The authors gratefully acknowledge X. Wu for providing the address of the Parihaka-3D data set.

## Data and materials availability

Data associated with this research are available and can be obtained by contacting the corresponding author.

## References

- Achanta, R., A. Shaji, K. Smith, A. Lucchi, P. Fua, and S. Süsstrunk, 2012, SLIC superpixels compared to state-of-the-art superpixel methods: *IEEE Transactions on Pattern Analysis and Machine Intelligence*, **34**, 2274–2282, doi: [10.1109/TPAMI.2012.120](https://doi.org/10.1109/TPAMI.2012.120).
- Alfarraj, M., Y. Alaudah, Z. Long, and G. AlRegib, 2018, Multi-resolution analysis and learning for computational seismic interpretation: *The Leading Edge*, **37**, 443–450, doi: [10.1190/tle37060443.1](https://doi.org/10.1190/tle37060443.1).
- Amin, A., and M. Deriche, 2015, A hybrid approach for salt dome detection in 2D and 3D seismic data: *IEEE International Conference on Image Processing*, 2537–2541.
- Aqrabi, A. A., T. H. Boe, and S. Barros, 2011, Detecting salt domes using a dip guided 3D Sobel seismic attribute: 81st Annual International Meeting, SEG, Expanded Abstracts, 1014–1018, doi: [10.1190/1.3627377](https://doi.org/10.1190/1.3627377).
- Balasubramanian, M., and E. L. Schwartz, 2002, The isomap algorithm and topological stability: *Science*, **295**, 7, doi: [10.1126/science.295.5552.7a](https://doi.org/10.1126/science.295.5552.7a).
- Berthelot, A., A. H. S. Solberg, and L. J. Gelius, 2013, Texture attributes for detection of salt: *Journal of Applied Geophysics*, **88**, 52–69, doi: [10.1016/j.jappgeo.2012.09.006](https://doi.org/10.1016/j.jappgeo.2012.09.006).
- Bo, H., F. L. Ma, and L. C. Jiao, 2006, Research on computation of GLCM of image texture: *Acta Electronica Sinica*, **1**, no. 1, 155–158.
- Bond, S. R., A. Hoeffler, and J. Temple, 2001, GMM estimation and empirical growth models: *Economics Papers*, **159**, 99–115.
- Boustani, B., A. Javaherian, M. Nabi-Bidhendi, S. Torabi, and H. R. Amindavar, 2019, Mapping channel edges in seismic data using curvelet transform and morphological filter: *Journal of Applied Geophysics*, **160**, 57–68, doi: [10.1016/j.jappgeo.2018.11.004](https://doi.org/10.1016/j.jappgeo.2018.11.004).
- Boykov, Y. Y., and M. P. Jolly, 2001, Interactive graph cuts for optimal boundary & region segmentation of objects in N-D images: *IEEE International Conference on Computer Vision*, 105–112.
- Cha, J., A. Henn, M. Stoddard, and A. Amini, 2018, 3D segmentation of the ascending and descending aorta from CT data via graph-cuts: *Medical Imaging 2018: Biomedical applications in molecular, structural, and functional imaging*, 105781R.
- Chen, H., C. Zhao, Z. Shi, and F. Zhu, 2018, An image splicing localization algorithm based on SLIC and image features: *Pacific Rim Conference on Multimedia*, 608–618.
- Chen, X., and U. Bagci, 2011, 3D automatic anatomy segmentation based on iterative graph-cut-ASM: *Medical Physics*, **38**, 4610–4622, doi: [10.1118/1.3602070](https://doi.org/10.1118/1.3602070).
- Chia, Y. K., C. P. Lee, and S. Z. Lo, 2014, Identifications of channel systems using coherence and spectral decomposition in offshore northwestern Australia: 84th Annual International Meeting, SEG, Expanded Abstracts, 2698–2702, doi: [10.1190/segam2014-1427.1](https://doi.org/10.1190/segam2014-1427.1).
- Córdoba, M., C. Bruno, M. Balzarini, and J. L. Costa, 2012, Principal component analysis with georeferenced data: An application in precision agriculture: *Revista De La Facultad De Ciencias Agrarias*, **44**, 27–39.
- Di, H., M. A. Shafiq, and G. AlRegib, 2017, Seismic-fault detection based on multiattribute support vector machine analysis: 87th Annual International Meeting, SEG, Expanded Abstracts, 2039–2044, doi: [10.1190/segam2017-17748277.1](https://doi.org/10.1190/segam2017-17748277.1).
- Fenster, A., and B. Chiu, 2005, Evaluation of segmentation algorithms for medical imaging: *International Conference of the IEEE Engineering in Medicine and Biology Society*, 7186–7189.
- Kadlec, B. J., G. A. Dorn, and H. M. Tufo, 2008, Confidence and curvature-guided level sets for channel segmentation: 78th Annual International Meeting, SEG, Expanded Abstracts, 879–883, doi: [10.1190/1.3063781](https://doi.org/10.1190/1.3063781).
- Karbalaali, H., A. Javaherian, S. Dahlke, and S. Torabi, 2017, Channel boundary detection based on 2D shearlet transformation: An application to the seismic data in the South Caspian Sea: *Journal of Applied Geophysics*, **146**, 67–79, doi: [10.1016/j.jappgeo.2017.09.001](https://doi.org/10.1016/j.jappgeo.2017.09.001).
- Kitrungrotsakul, T., Y. W. Chen, X. H. Han, and L. F. Lin, 2015, Supervoxels based Graph cut for Medical Organ segmentation: *IFAC-PapersOnLine*, **48**, 70–75, doi: [10.1016/j.ifacol.2015.10.117](https://doi.org/10.1016/j.ifacol.2015.10.117).
- Le, Y. X., and Y. G. Wang, 2002, Nonparametric regression applied in porosity parameter prediction: *Geological Science*, **37**, 118–126.
- Lin, X., B. Cowan, and A. Young, 2006, Model-based Graph Cut method for segmentation of the left ventricle: *International Conference of the IEEE*, 3059–3062.
- Liu, X. F., X. D. Zheng, G. C. Xu, L. Wang, and H. Yang, 2010, Locally linear embedding-based seismic attribute extraction and applications: *Applied Geophysics*, **7**, 365–375, doi: [10.1007/s11770-010-0260-2](https://doi.org/10.1007/s11770-010-0260-2).
- Liu, Z. N., C. Y. Song, Z. Y. Li, X. M. Yao, and G. M. Hu, 2016, 3D modeling of geological anomalies based on segmentation of multiattribute fusion: *Applied Geophysics*, **13**, 519–528, doi: [10.1007/s11770-016-0579-4](https://doi.org/10.1007/s11770-016-0579-4).
- Long, Z., Y. Alaudah, M. A. Qureshi, Y. Hu, Z. Wang, M. Alfarraj, G. AlRegib, A. Amin, M. Deriche, S. Al-Dharrab, and H. Di, 2018, A comparative study of texture attributes for characterizing subsurface structures in seismic

- volumes: Interpretation, **6**, no. 4, T1055–T1066, doi: [10.1190/INT-2017-0181.1](https://doi.org/10.1190/INT-2017-0181.1).
- Mathewson, J., and D. Hale, 2009, Detection of channels in seismic images using the steerable pyramid: 79th Annual International Meeting, SEG, Expanded Abstracts, 199–210, doi: [10.1190/1.3063777](https://doi.org/10.1190/1.3063777).
- Pham, N., S. Fomel, and D. Dunlap, 2018, Automatic channel detection using deep learning: 88th Annual International Meeting, SEG, Expanded Abstracts, 2026–2030, doi: [10.1190/segam2018-2991756.1](https://doi.org/10.1190/segam2018-2991756.1).
- Qi, X. M., and S. C. Zhang, 2012, Application of seismic multi-attribute fusion method based on D-S evidence theory in prediction of CBM-enriched area: Applied Geophysics, **9**, 80–86, doi: [10.1007/s11770-012-0317-5](https://doi.org/10.1007/s11770-012-0317-5).
- Shafiq, M. A., Z. Wang, A. Amin, H. Tamir, D. Mohamed, and A. Ghassan, 2015, Detection of salt-dome boundary surfaces in migrated seismic volumes using gradient of textures: 85th Annual International Meeting, SEG, Expanded Abstracts, 1811–1815, doi: [10.1190/segam2015-5927230.1](https://doi.org/10.1190/segam2015-5927230.1).
- Shi, P., S. Yuan, T. Wang, Y. Wang, and T. Liu, 2018, Fracture identification in a Tight Sandstone reservoir: A seismic anisotropy and automatic multisensitive attribute fusion framework: IEEE Geoscience and Remote Sensing Letters, 1–5.
- Suarez, Y., K. J. Marfurt, and M. Falk, 2008, Seismic attribute-assisted interpretation of channel geometries and infill lithology: A case study of Anadarko basin Red Fork channels: 78th Annual International Meeting, SEG, Expanded Abstracts, 963–967, doi: [10.1190/1.3063798](https://doi.org/10.1190/1.3063798).
- Tian, Z., L. Z. Liu, and B. Fei, 2015, A supervoxel-based segmentation method for prostate MR images: Proceedings of SPIE — The International Society for Optical Engineering, **9413**, 941318.
- Varini, C., A. Degenhard, and T. Nattkemper, 2005, ISOLLE: Locally linear embedding with geodesic distance: European Conference on Principles and Practice of Knowledge Discovery in Databases, 331–342.
- Varini, C., A. Degenhard, and T. W. Nattkemper, 2006, ISOLLE: LLE with geodesic distance: Neurocomputing, **69**, 1768–1771, doi: [10.1016/j.neucom.2005.12.120](https://doi.org/10.1016/j.neucom.2005.12.120).
- Veksler, O., Y. Boykov, and P. Mehrani, 2010, Superpixels and supervoxels in an energy optimization framework: Proceedings of the European Conference on Computer Vision, 211–224.
- Wang, S., H. Lu, and F. Yang, 2011, Superpixel tracking: International Conference on Computer Vision, 1323–1330.
- Wu, H., J. Li, H. Liu, Y. Li, and Y. Zou, 2018, Application of seismic multi attribute fusion technology in reservoir rediction of Baer Depression: IOP Conference Series: Materials Science and Engineering, 012003.
- Wu, X., 2017, Directional structure-tensor-based coherence to detect seismic faults and channels: Geophysics, **82**, no. 2, A13–A17, doi: [10.1190/geo2016-0473.1](https://doi.org/10.1190/geo2016-0473.1).
- Wu, X., and Z. Guo, 2019, Detecting faults and channels while enhancing seismic structural and stratigraphic features: Interpretation, **7**, no. 1, T155–T166, doi: [10.1190/INT-2017-0174.1](https://doi.org/10.1190/INT-2017-0174.1).
- Zhang, J. H., L. Zhen, B. H. Zhu, D. Y. Feng, M. Z. Zhang, and X. F. Zhang, 2011, Fluvial reservoir characterization and identification: A case study from Laohekou Oilfield: Applied Geophysics, **8**, 181–188, doi: [10.1007/s11770-011-0288-y](https://doi.org/10.1007/s11770-011-0288-y).
- Zhou, J., Y. Zhang, Z. Chen, and J. H. Li, 2007, Detecting boundary of salt dome in seismic data with edge detection technique: 77th Annual International Meeting, SEG, Expanded Abstracts, 1392–1396, doi: [10.1190/1.2792759](https://doi.org/10.1190/1.2792759).

---

Biographies and photographs of the authors are not available.